Open-loop and closed-loop control of flying qubits

M Lucamarini, G Di Giuseppe, D Vitali, P Tombesi

Open-loop and Closed-loop Control of Flying Qubits

M. Lucamarini[1,2], G. Di Giuseppe[1,2], D. Vitali[1], and P. Tombesi[1,2]

[1] School of Science and Technology, Physics Division, University of Camerino, I-62032 Camerino (MC), Italy.

[2] CriptoCam S.r.l., via Madonna delle Carceri 9, I-62032 Camerino (MC), Italy.

Abstract. We describe two recent techniques, along with related experiments, to control and reduce the noise affecting a photon polarization qubit. The first is based on the open-loop "bang-bang" method, where suitably tailored pulses are implemented on the system to adverse polarization decoherence. This requires only passive elements when the physical system is a photon and the operation are performed in space rather than in time. The second technique is based on a closed-loop "asymmetric feedback", where some quantities are measured and used for a real-time correction of the system dynamics. This technique necessarily requires an active electronics to work.

1. Introduction

The use of photons as physical systems to transmit information over long distances is widespread in telecommunications, mainly because of the low loss-coefficient pertaining to this kind of transmissions, both in optical fibres [1] and in free space [2].

A light pulse often requires a precise definition of its state of polarization, especially when it carries the information exchanged between two distant users. This in particular holds true when single photons are used in the communication, each one carrying one bit of information. In this case the photon's quantum nature defines a "quantum bit" or *qubit*, which is protected against undesired intrusions [3, 4].

The initial state of polarization can be usually very well prepared. However it is much more demanding to maintain this state along the communication channel, and to align the final detection stage in the same direction as the preparation stage, so to allow for a reliable measurement [5].

In this paper we describe two techniques to reliably transmit and detect the quantum information encoded in polarization qubits. One prominent feature of this problem, and a relevant difference respect to the classical scenario, is that at least two *non-orthogonal* states of polarization must be reliably transmitted. In fact, the reliable transmission of a single state of polarization or of two orthogonal states of polarization, like required in a classical communication setting, is not sufficient to guarantee the unconditional security of the communication, which is the main motivation for using quantum information.

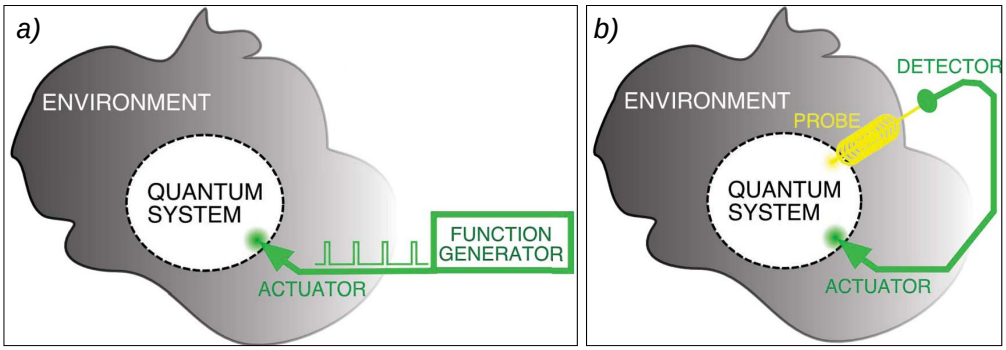

Figure 1. (Color online) Strategies for protecting quantum system against decoherence: a) open-loop controls, based on external, suitably tailored, time-dependent driving chosen such to eliminate undesired effect of the environment. b) closed-loop techniques, based on measurements and consequent real-time correction of the system dynamics.

Quite often, to have a faithful transmission of two non-orthogonal polarization states is tantamount to have a faithful transmission of *any* polarization state. In fact, two orthogonal polarizations define a basis, which can be chosen to coincide with the eigenbasis set forth by the noise itself. The quantum state prepared in this particular basis can then travel unaffected by the noise, in a sort of "noise-free environment". On the contrary, when at least two non-orthogonal polarizations are involved, no trivial noise-free subspace is available, and it becomes necessary to adverse the noise regardless of the polarization basis of the qubit. This problem is then more demanding than the classical one.

The first technique discussed in this paper is devised specifically to preserve the coherence of a polarization qubit against the detrimental effects of a general noise encountered in the communication channel. It is an *open-loop control*, where the system is subject to external, suitably tailored, time-dependent pulses which do not require any measurement (see left inset of Fig. 1). The control operations are chosen so that any undesired effect of the environment, such as dissipation, decoherence, heating, can be eliminated if the controls are applied faster than the environment correlation time. The physical idea behind these open-loop schemes comes from refocusing techniques in NMR spectroscopy [6] where they are typically implemented in time via strong and rapid pulses known as "bang-bang" (BB) controls. However open-loop decoupling strategies have been suggested in various physical contexts: to inhibit the decay of an unstable atomic state [7, 8], to suppress the magnetic state decoherence [9] and the heating in ion traps [10], to contrast the quantum noise due to scattering processes [11] and the polarization mode dispersion [12] in optical fibers. BB control has been first demonstrated in NMR systems (see e.g. [13]). Then, it has been proven with nuclear spin qubits in fullerene [14], nuclear-quadrupole qubits [15] and very recently also with electron spins in Penning traps [16] and with polarization qubits in a plane-parallel cavity [17] and in a ring cavity [18]. We will describe and discuss these last experiments

in some detail.

The second technique is an example of *closed-loop control* [19], where the polarization qubit is subject to appropriate measurements, whose results are then used for a real-time correction of the system dynamics (see right inset of Fig. 1). In this case we discuss two recent, different, experiments reported in [20] and in [21]. The former is based on a standard feedback, where the receiver transmits to the sender some (classical) information in order to allow a better encoding of the initial state. The latter is rather a *feed-forward* technique, where the receiver has to modify the measuring apparatus so to match a given set-point; this is entirely local to the receiver and does not require any exchange of information with the transmitter. In the following, we refer to both techniques as to "feedback", specifying the differences between the two when they are substantial.

The presented feedback aims to correct some forms of noise affecting the quantum states of light and in particular their polarization. Note that by "real-time" we do not mean "in a single shot". In fact, the feedback correction is driven by the average value of N independent measurements that are collected and analyzed on a statistical basis. These measurements are intrinsically quantum, as they are performed on single-photon polarization states of light, selected to be non-orthogonal to each other. The classical limit is obtained when several photons populate the states. This redundancy makes the informative states more orthogonal and therefore more distinguishable; in turn this allows for a more reliable communication and a better control of the channel noise, as it always happens in classical communications, at the expenses of the quantum features of the transmission. For example, the security entailed by the nonorthogonality condition is entirely suppressed by a redundant encoding.

2. Open-loop control through passive optical elements

In this section we initially introduce our noise model for the polarization qubit. Then we consider the experiments reported in [17] and [18], where photons were made circulate in optical cavities, and apply to this situation our formalism. In this case polarization decoherence is synthetically introduced in the experiment through the polarization dispersive properties of the cavity elements. Finally we show how to reestablish the coherence of the polarization qubits using the open-loop control.

2.1. The noise model

Our noise model is purposely constructed close to the experimental implementations described later on in the paper. It takes into account the dispersive properties of an optical cavity passive elements, like mirrors, crystals and waveplates. In such devices there is an intrinsic dependence upon both polarization and frequency which realizes an effective coupling between the two degrees of freedom of the photon. Moreover the detection of the final polarization state is inevitably performed through a detector

which has a nonzero integration time. Hence the resulting measurement traces out the frequency degree of freedom. If the initial field is not monochromatic, all the information transferred from the polarization modes to the frequency modes goes lost, inducing on the polarization qubit a decoherence in the form of a dephasing process. Besides representing the proper description of the experimental scenario, our noise model can, to a certain extent, account for the real propagation of the light in a dispersive medium like, e.g., an optical fibre. Of course this is true until the real propagator between two consecutive optical elements in the dispersive medium resembles the free-space propagator considered here.

Let's then consider the following initial pure state, the product of a general polarization state and a general frequency state:

$$|\pi\rangle_{in} \otimes |\omega\rangle_{in} = \sum_{i=0,1} \alpha_i |\pi_i\rangle \otimes \int d\omega \mathcal{E}(\omega) |\omega\rangle \tag{1}$$

with $|\pi_0\rangle$ ($|\pi_1\rangle$) the positive (negative) eigenstate of the Pauli matrix $\sigma_Z = \mathbb{Z}$, corresponding to the Horizontal (Vertical) polarization with respect to the main plane of the experiment; α_i complex coefficients satisfying the completeness relation $\sum_{i=0,1} |\alpha_i|^2 = 1$; $|\omega\rangle$ a frequency eigenstate and $\mathcal{E}(\omega)$ a distribution of the frequency eigenvalues satisfying the completeness relation $\int d\omega |\mathcal{E}(\omega)|^2 = 1$. One such distribution is the Gaussian:

$$\mathcal{E}(\omega) = \frac{1}{\sqrt[4]{\pi\sigma_\omega^2}} \exp\left[-(\omega-\omega_0)^2 / \left(2\sigma_\omega^2\right)\right]. \tag{2}$$

The initial qubit state in Eq. (1) can be approximately obtained by an attenuated laser pulse injected into a cavity after a careful selection of its polarization state, and eventually detected through a frequency-insensitive single-photon detector [18, 22]. Hence, such a state is suitable to describe the experiments discussed later on in this paper.

As mentioned, a frequency-insensitive measurement leads to trace out the frequency degree of freedom. However, since the polarization and the frequency are factorized, this operation still restitutes a pure polarization state when effected on the initial state of Eq. (1):

$$\begin{aligned}
\rho_P &= \int d\omega' \langle\omega'| \left(|\pi\rangle_{in} |\omega\rangle_{in} \otimes_{in} \langle\omega|_{in} \langle\pi|\right) |\omega'\rangle \\
&= \left(\sum_{i,j} \alpha_i \alpha_j^* |\pi_i\rangle \langle\pi_j|\right) \left(\int d\omega |\mathcal{E}(\omega)|^2\right) \\
&= \sum_{i,j} \alpha_i \alpha_j^* |\pi_i\rangle \langle\pi_j| = |\pi\rangle_{in} \langle\pi|.
\end{aligned}$$

When noise acts on the qubit this ceases to be true. The noise entangles the polarization and frequency degrees of freedom. The typical element realizing such coupling is a dispersive wave retarder, which can be written by the following Jones

matrix:

$$\mathbb{M}_{\mathbb{Z}}(\omega) = \begin{pmatrix} e^{-i\phi_0(\omega)} & 0 \\ 0 & -e^{-i\phi_1(\omega)} \end{pmatrix} = \mathbb{Z}, \exp\left[-i\phi(\omega)\mathbb{Z}\right], \tag{3}$$

with $\phi(\omega) = \phi_0(\omega) - \phi_1(\omega)$ the relative phase angle accumulated by the qubit after a single passage through the dispersive element. This angle depends upon both polarization and frequency, and can thus entangle the two degrees of freedom. Hence when $\mathbb{M}_{\mathbb{Z}}(\omega)$ acts on a pure state like that in Eq. (1) the state becomes:

$$\begin{aligned} \rho' &= M_Z(\omega)\left(|\pi\rangle_{in}\langle\pi| \otimes |\omega\rangle_{in}\langle\omega|\right) M_Z^{\dagger}(\omega) \\ &= \int d\omega \left|\mathcal{E}(\omega)\right|^2 |\omega\rangle\langle\omega| \otimes \begin{pmatrix} |\alpha_0|^2 & -e^{-i\phi(\omega)}\alpha_0\alpha_1^* \\ -e^{i\phi(\omega)}\alpha_0^*\alpha_1 & |\alpha_1|^2 \end{pmatrix} \end{aligned}$$

and after the trace on the frequency degree of freedom we obtain:

$$\rho'_P = \begin{pmatrix} |\alpha_0|^2 & -\alpha_0\alpha_1^* \int d\omega \left|\mathcal{E}(\omega)\right|^2 e^{-i\phi(\omega)} \\ -\alpha_0^*\alpha_1 \int d\omega \left|\mathcal{E}(\omega)\right|^2 e^{i\phi(\omega)} & |\alpha_1|^2 \end{pmatrix}.$$

This state is no longer pure because of the presence of the terms $e^{\pm i\phi(\omega)}$ in the off-diagonal frequency integral. To see this one can expand $\phi(\omega)$ to the first order like $\phi(\omega) = \phi_0 + \omega\tau$. The off-diagonal term $(\rho'_P)_{12}$ then becomes (the other term $(\rho'_P)_{21}$ is analogous):

$$(\rho'_P)_{12} = -\alpha_0\alpha_1^* e^{-i\phi_0} \int d\omega \left|\mathcal{E}(\omega)\right|^2 e^{-i\omega\tau}.$$

The integral is the Fourier transform of the function $\left|\mathcal{E}(\omega)\right|^2$. If we think to the simple case of the Gaussian of Eq. (2), then the Fourier transform is still a Gaussian, in the time domain, whose width is $\Delta\tau \sim \frac{1}{\sigma_\omega}$; hence, after the amount of time $\Delta\tau$ the off-diagonal term will be less than half its initial value.

The effect becomes more evident when the noise operator $\mathbb{M}_{\mathbb{Z}}(\omega)$ is applied n times to the qubit, because the angle $\phi(\omega)$ is replaced by $n\phi(\omega)$ and the typical decay time $\Delta\tau$ becomes $\Delta\tau/n$. This typically happens when the qubit is circulating inside an optical cavity as it meets the same optical elements several times before being detected.

The basic structure of the noise $\mathbb{M}_{\mathbb{Z}}(\omega) = \mathbb{Z}\exp\left[-i\phi(\omega)\mathbb{Z}\right]$ can be generalized considerably in order to include all possible transformations on a polarization qubit. The most general operator can be written as follows:

$$\mathbb{N}(\omega,\theta) = \exp\left[-i\gamma_{\omega,\theta}\left(\overrightarrow{s}_{\omega,\theta}\cdot\overrightarrow{\sigma}\right)\right] \tag{4}$$

with $\gamma_{\omega,\theta}$ a real parameter, $\overrightarrow{s}_{\omega,\theta} = \left[s_X(\omega,\theta), s_Y(\omega,\theta), s_Z(\omega,\theta)\right]$ the vector of the direction cosines, and $\overrightarrow{\sigma} = (\sigma_X, \sigma_Y, \sigma_Z) = (\mathbb{X}, \mathbb{Y}, \mathbb{Z})$ the vector of the Pauli matrices. Such a generalized noise operator includes the noise encountered by the polarization qubit during the propagation in a birefringent medium like an optical fibre, usually known as "polarization mode dispersion" [12]. Hence, the experiments discussed here are representative of the dynamics of a polarization qubit traveling inside an optical fibre.

The generalized noise operator of Eq. (4) can be experimentally obtained by rotating the main axis of the element generating $\mathbb{M}_{\mathbb{Z}}(\omega)$ by an angle θ around an axis different from $\mathbb{Z}$, for instance around $\mathbb{X}$. We can define the following rotation around $\mathbb{X}$:

$$\mathbb{B}_{\mathbb{X}}(\theta) = \exp(-i\theta\mathbb{X})$$

and then obtain:

$$\begin{aligned}\mathbb{N}(\omega,\theta) &= \mathbb{M}_{\mathbb{Z}}(\omega) \circ \mathbb{B}_{\mathbb{X}}(\theta) \\ &= \mathbb{Z}\exp[-i\phi(\omega)\mathbb{Z}]\exp(-i\theta\mathbb{X}) \\ &= -i\exp[-i\gamma_{\omega,\theta}(\overrightarrow{s}_{\omega,\theta}\cdot\overrightarrow{\sigma})]\end{aligned}$$

with $\gamma_{\omega,\theta}$ defined by:

$$\cos\gamma_{\omega,\theta} = \cos\theta\sin\phi(\omega)$$

and $\overrightarrow{s}_{\omega,\theta}$ defined by the following direction cosines:

$$\begin{aligned}s_X(\omega,\theta) &= [\sin\theta\sin\phi(\omega)]/[\sin\gamma_{\omega,\theta}], \\ s_Y(\omega,\theta) &= [-\sin\theta\cos\phi(\omega)]/[\sin\gamma_{\omega,\theta}], \\ s_Z(\omega,\theta) &= [-\cos\theta\cos\phi(\omega)]/[\sin\gamma_{\omega,\theta}].\end{aligned}$$

The polarization decoherence just described can be inhibited by means of an open-loop dynamical decoupling known as "bang-bang" (BB). The term describes a technique, introduced for the first time in the Nuclear Magnetic Resonance (NMR) spectroscopy [6], where a series of suitably tailored pulses are shot on the qubit to alter its dynamics and decouple it from the surrounding environment. Usually the pulses are supposed to be very short and intense, and applied faster than the typical environment time-scale. In NMR the pulses are implemented in time through a sequence of RF modulation of an external magnetic field. In the case of a photon the pulses are implemented in space, i.e., along the photon path, by means of suitably oriented waveplates. Due to the very short time of flight of the photon inside the optical elements, the BB approximation holds very well in this situation.

The first proof-of-principle of the BB impulsive dynamics in the optical domain was given in [17], by using optical pulses traveling back-and-forth in a plane-parallel cavity. That experiment clearly demonstrated that BB can be applied to light pulses traveling on a two-way optical channel [23]. On the other hand, in Ref. [18], the BB is applied to the evolution of an optical pulse circling in a triangular ring cavity. In this case the light pulse always travels in the forward direction, thus extending the applicability of BB to one-way channels too, like optical fibres. As already mentioned, the caveat is that the extension to a dispersive medium like an optical fibre can work as long as the light propagator encountered in the fibre between two consecutive BB operations is similar to the free-space propagator considered here. This assumption sounds reasonable when both the beat length and the mode coupling length of the fibre, presently about 10 meters, are much bigger than the distance between consecutive BB controls [12].

2.2. Bang-bang controls in a plane-parallel cavity

In this section we apply our formalism to the experiments performed in Ref. [17], which represent the first proof-of-principle of the BB dynamics in the optical domain. In this case the polarization qubit travels in a plane-parallel optical cavity and both the noise and the BB controls are introduced by means of passive optical elements. In this setting polarization decoherence occurs because of the reflection on the cavity mirrors, which depend on both frequency and polarization. After a few cavity round trips, the initially pure polarization state becomes highly mixed. On the contrary, after inserting appropriate waveplates in the cavity realizing an effective impulsive BB, polarization decoherence is significantly inhibited [17].

The experimental configuration consists in a 50 cm plane-parallel cavity with one or more rotating elements between the two mirrors. Attenuated light pulses are generated by a diode laser of central wavelength $\lambda = 670$ nm. Their bandwidth is fixed at $\Delta\lambda = 10$ nm or $\Delta\lambda = 1.5$ nm depending on the experimental conditions. The polarization states enter the cavity from one mirror and emerge, after about 10 round trips, either from the second mirror or from a thin glass placed in the center of the cavity. Finally, the polarization of those pulses which completed two round trips is analyzed to look for an effect similar to the BB compensation. We remark that the only pulses analyzed are those which have traveled an *even* number of times in the same path.

In the *first experiment* of Ref. [17] the main sequence of operators acting on the flying qubit can be obtained starting from the output mirror and listing down all the operators encountered by the photon in the cavity before it meets the output mirror a second time.

Initially we ignore the optical element in the setup implementing the BB control. The noise is given in the form of Eq. (3) by a PBS-based Michelson interferometer aligned along the $\mathbb{Z}$ direction, with one arm slightly longer than the other. It can be represented by the operator:

$$\mathbb{M}_{\mathbb{Z}} = \exp\left(i\phi\mathbb{Z}\right), \tag{5}$$

where ϕ depends upon the unbalance of the interferometer. After n cycles in the cavity we have the following sequence of operators:

$$\mathbb{U}_{fe}^{(n)} = \left[\mathbb{Z}\left(\mathbb{Z}\mathbb{M}_{\mathbb{Z}}\mathbb{Z}\right)^{T}\mathbb{Z}\mathbb{M}_{\mathbb{Z}}\right]^{n} = \left(\mathbb{M}_{\mathbb{Z}} \circ \mathbb{M}_{\mathbb{Z}}\right)^{n}. \tag{6}$$

In the first line we used the label *fe* to indicate the free evolution of the photon, i.e. without the BB control applied. In the operator equation we inserted $\mathbb{Z}$ and transposition operations according to the standard description of reflection at the interface between two media [24]. It prescribes that every operator met by the photon in the "real" space is listed down with its standard representation, while every operator met by the photon in the "mirrored" space, i.e. after an odd number of reflections, is written by inserting its Jones matrix between two $\mathbb{Z}$ operations and then transposed [24]. In the second line of Eq. (6) we also used the standard properties of the Pauli matrices.

It can be seen that in this case the noise accumulates together with the passages of the photon in the cavity.

Let's consider now the insertion of a BB element in the plane-parallel cavity, represented by a $\lambda/4$ wave-plate oriented at 45° from the horizontal plane, before the optical element corresponding to the noise of Eq. (5). Such an element corresponds to the following operator:

$$\mathbb{R} = (\mathbb{I} + i\mathbb{X})/\sqrt{2} \tag{7}$$

With this element in place the new operator sequence becomes:

$$\begin{aligned}\mathbb{U}_{bb}^{(n)} &= \left\{\mathbb{Z}\left[(\mathbb{Z}\mathbb{M}_{\mathbb{Z}}\mathbb{Z})(\mathbb{Z}\mathbb{R}\mathbb{Z})\right]^T \mathbb{Z}(\mathbb{M}_{\mathbb{Z}}\mathbb{R})\right\}^n \\ &= (i)^n \mathbb{R}\left(\mathbb{M}_{\mathbb{Z}}\mathbb{X}\mathbb{M}_{\mathbb{Z}}^{-1}\right)^n \mathbb{R}^{-1}.\end{aligned}$$

In this case, the label *bb* indicates we applied the BB controls. When we consider an even number of round trips we obtain:

$$\mathbb{U}_{bb}^{2n} = (-)^n \mathbb{I},$$

i.e. an operator proportional to the identity. This means that decoherence is completely suppressed after every even number of round-trips.

Let's have a closer look at the main operator sequence repeated in each cycle:

$$\mathbb{M}_{\mathbb{Z}}\mathbb{X}\mathbb{M}_{\mathbb{Z}}^{-1}. \tag{8}$$

The first term is the noise operator. The second term comes from the rotating element, and the third term is the inverse of the noise operator, which is given by the recycling mirror at the end of the cavity. That mirror is essential for the noise compensation: it executes a time-reversal on the photon, forcing it to retrace on the backward path the same steps it traced on the forward path. This is somewhat similar to the *retracing beam* effect (RB), where a light pulse traveling back and forth between two mirrors reverts on every "backward path" the dephasing introduced by dispersive elements during each "forward path" [23]. The RB compensation technique can only work on a two-way channel.

In the *second experiment* of Ref. [17] the rotating element is a $\lambda/2$ wave-plate whose operator is $i\mathbb{X}$. This time there are two kinds of noise: one from the same Michelson interferometer of the first experiment, described by $\mathbb{M}_{1\mathbb{Z}} = \exp(i\phi_1\mathbb{Z})$, and one from a birefringent quartz crystal with optical axis parallel to the interferometer, described by $\mathbb{M}_{2\mathbb{Z}} = \exp(i\phi_2\mathbb{Z})$.

In this case we write directly the operator sequence pertaining to the compensated dynamics. The non-compensated dynamics can be easily obtained from the compensated one by removing the operators corresponding to BB controls, i.e. the operator $\mathbb{R}$. The main operator sequence is then:

$$\begin{aligned}\mathbb{U}_{bb}^{n} &= \left\{\mathbb{Z}\left[(\mathbb{Z}\mathbb{M}_{1\mathbb{Z}}\mathbb{Z})(\mathbb{Z}\mathbb{R}\mathbb{Z})(\mathbb{Z}\mathbb{M}_{2\mathbb{Z}}\mathbb{Z})\right]^T \mathbb{Z}(\mathbb{M}_{1\mathbb{Z}}\mathbb{R}\mathbb{M}_{2\mathbb{Z}})\right\}^n \\ &\propto \left[\left(\mathbb{M}_{1\mathbb{Z}}^{-1}\mathbb{M}_{2\mathbb{Z}}\right)\left(\mathbb{M}_{1\mathbb{Z}}^{-1}\mathbb{M}_{2\mathbb{Z}}\right)\right]^n = \exp\left[i(\phi_2 - \phi_1)n\mathbb{Z}\right],\end{aligned}$$

which entails a suppression of decoherence which depends upon the phase difference $(\phi_1 - \phi_2)$. This phase difference appears in the exponent because of the term $\mathbb{M}_{1\mathbb{Z}}^{-1}$ in the operator sequence, which indicates a time-inversion in the compensation process. This experiment showed only a partial compensation of decoherence because the phase difference is canceled only approximately.

In the *third experiment* of Ref. [17] the rotating element is a quartz plate with optical activity, performing the operation $\mathbb{Y}$. As in the second experiment there are two kinds of noise, but this time they are given by two birefringent crystals, of width 0.8 mm and 1.0 mm, oriented at $-10°$ from the horizontal plane. Their operators are $\mathbb{M}_1 = \mathcal{R}\exp(i\phi_1\mathbb{Z})\mathcal{R}^{-1}$ and $\mathbb{M}_2 = \mathcal{R}\exp(i\phi_2\mathbb{Z})\mathcal{R}^{-1}$, with $\mathcal{R}$ a $(-10°)$-rotation from the horizontal axis. After $2n$ cycles the compensated sequence operator is:

$$\begin{aligned}\mathbb{U}_{bb}^{n} &= \left\{\mathbb{Z}\left[(\mathbb{Z}\mathbb{M}_2\mathbb{Z})(\mathbb{Z}\mathbb{R}\mathbb{Z})(\mathbb{Z}\mathbb{M}_1\mathbb{Z})\right]^T\mathbb{Z}(\mathbb{M}_2\mathbb{R}\mathbb{M}_1)\right\}^n \\ &\propto \left[\mathbb{M}_{12}\mathbb{Y}\mathbb{M}_{12}^{-1}\mathbb{Y}\right]^n, \end{aligned} \tag{9}$$

where $\mathbb{M}_{12} = \mathbb{M}_1 \circ \mathbb{M}_2^{-1}$. The input light in this experiment is linearly polarized at 35° from the horizontal axis, thus making an angle of 45° with the axis of $\mathcal{R}$. This is analogous to a 45° polarization that meets a noise along $\mathbb{Z}$, like in the second experiment. Furthermore the rotating element $\mathbb{Y}$ acts equally good on any linear input polarization. Hence $\mathbb{M}_i = \mathbb{M}_{i\mathbb{Z}} = \exp(i\phi_i\mathbb{Z})$, with $i = \{1, 2\}$, and

$$\begin{aligned}\mathbb{U}_{bb}^{n} &\propto \left\{\exp\left[i(\phi_2 - \phi_1)\mathbb{Z}\right]\mathbb{Y}\exp\left[-i(\phi_2 - \phi_1)\mathbb{Z}\right]\mathbb{Y}\right\}^n \\ &= \exp\left[2i(\phi_2 - \phi_1)n\mathbb{Z}\right], \end{aligned}$$

with a partial compensation of the noise analogous to what obtained in the second experiment. Note that the structure of the main operator sequence, Eq. (9), shows again a time-inversion entailed by the recycling mirror of the plane-parallel cavity.

Finally, the *fourth experiment* in Ref. [17] includes a noise configuration in which $\mathbb{M}_1 = \exp(i\phi_1\mathbb{Z})$ and $\mathbb{M}_2 = \mathcal{R}\exp(i\phi_2\mathbb{Z})\mathcal{R}^{-1}$, where $\mathcal{R}$ is the same rotation as before. As a consequence, the structure of the noise is the same as in Eq. (9).

2.3. Bang-bang controls in a ring cavity

In this section we discuss three experiments reported in [18]. In the first, the polarization decoherence is inhibited through the simple "Carr-Purcell" decoupling scheme [25, 26, 27], which is a particular case of BB control realized by adding a single wave-plate within the cavity, suitably oriented. In the second the more general Pauli-group decoupling [27] is used, which is realized by employing *two* waveplates with orthogonal rotation axes and we show that polarization decoherence is inhibited also in this case. In the third and final experiment the ring cavity is modified in order to implement the most general form of decoherence acting on the polarization qubit. This is implemented by placing a Soleil–Babinet (SB) compensator with axis at 45° with respect to the cavity plane in front of each plane mirror.

The experimental apparatus of Ref. [18] is composed by a laser diode with central wavelength at $\lambda_0 \simeq 800$ nm and bandwidth $\Delta\lambda \simeq 15$ nm, pulsed at repetition rate of

100 KHz and with pulse duration ∼100 ps. The laser is attenuated and injected in a triangular ring cavity through a spherical mirror with radius of curvature 1 m and reflectivity ∼ 98%. The cavity is also formed by two flat mirrors at 45° with reflectivity $\gtrsim$ 99%. The aperture angle of the cavity at the spherical mirror is ∼ 8°. The long arms of the cavity are ∼ 0.94 m and the short arm is ∼ 0.13 m determining a total cavity length of ∼ 2.01 m. The polarization state of the laser is prepared by using a polarizing beam-splitter (PBS), a half-wave plate ($\lambda/2$) and a quarter-wave plate ($\lambda/4$) with a very high degree of purity. At every round trip the light is extracted from the cavity with 4% probability using a ∼100 μm thin glass plate. Its polarization is analyzed by means of the tomographic technique [28], and then sent into a multimode fiber connected to a single-photon detector with quantum efficiency ∼ 70%.

A cavity mirror generally produces a phase shift which depends upon both frequency and polarization, and therefore its action is described by the matrix given in Eq. (4), with $\phi(\omega) = \phi_0(\omega) - \phi_1(\omega)$ the relative phase due to the polarization-reflectivity difference. The two plane mirrors at 45° can be assumed identical and are therefore characterized by the same matrix $\mathbb{M}_{\mathbb{Z}}(\omega)$. The third concave mirror of the cavity is almost at normal incidence: this mirror does not distinguish H and V polarization, so that $\phi(\omega) \simeq 0$ and therefore it acts as $\mathbb{M}_{\mathbb{Z}}(\omega) \simeq \mathbb{Z}$.

The polarization qubit in the cavity is subjected to a phase-noise along z-axis and the unitary operator describing the polarization transformation after one cavity round-trip for a given frequency component is given by

$$\begin{aligned} \mathbb{U}_{fe}[\phi(\omega)] &= \mathbb{Z} \cdot \mathbb{M}_{\mathbb{Z}}(\omega) \cdot \mathbb{M}_{\mathbb{Z}}(\omega) \\ &= \mathbb{Z} \exp\{-i2\phi(\omega)\mathbb{Z}\}\,, \end{aligned} \tag{10}$$

The dispersive properties of the two plane mirrors at 45°, i.e., their frequency dependence, generates polarization decoherence: in fact the frequency dependence of the matrix $\mathbb{M}_{\mathbb{Z}}$ appears only if the optical element is dispersive, otherwise it is constant and it does not entangle polarization and frequency degrees of freedom.

The BB dynamical decoupling is realized by adding two control operations within the cavity: i) a second $\mathbb{Z}$ wave-plate in the long arm of the cavity in addition to the one used for compensating the spherical mirror; ii) a Soleil–Babinet (S–B) compensator with axis at 45° with respect to the cavity plane and delay equal to $\lambda/2$ in the short arm of the cavity, acting therefore as $\mathbb{X}$. The two controls implement every two cavity round-trips the full Pauli-group decoupling for a polarization qubit [29, 12], and the overall transformation for a double round-trip is given by

$$\begin{aligned} \mathbb{U}_{bb}[\phi(\omega)] = &\ [\mathbb{Z}\mathbb{M}_{\mathbb{Z}}\mathbb{X}\mathbb{M}_{\mathbb{Z}}] \cdot [\mathbb{Z}\mathbb{M}_{\mathbb{Z}}\mathbb{X}\mathbb{M}_{\mathbb{Z}}] \\ &= [\mathbb{Z}\mathbb{X}]\,[\mathbb{Z}\mathbb{X}] = (i\mathbb{Y})^2 = -\mathbb{I}\,, \end{aligned} \tag{11}$$

where we have omitted the frequency dependence in the term $\mathbb{M}_{\mathbb{Z}}(\omega)$. Therefore the polarization transformation is proportional to the identity operator, thus implying a *perfect* preservation of every input polarization state, i.e., a complete suppression of decoherence. This is experimentally verified for H, D and R input polarizations. When

BB is not performed polarizations D and R decay to the fully unpolarized state, while H, being an eigenstate of $\mathbb{Z}$, is unaffected by decoherence. On the contrary, polarization decoherence is completely suppressed when BB is applied [18].

2.3.1. Carr–Purcell decoupling Polarization decoherence caused by a cavity round-trip acts along a known axis of the Bloch sphere, the z-axis, and therefore even a simpler decoupling scheme, namely the Carr-Purcell decoupling, suffices for suppressing decoherence. It is realized by inserting a single optical element in the cavity, represented by the operator $\mathbb{X}$, implemented by properly adjusting the S–B in the short arm of the cavity. The Carr-Purcell decoupling scheme requires again a double round-trip in the cavity, which gives the evolution

$$\mathbb{U}_{bb}[\phi(\omega)] = \mathbb{Z}\mathbb{M}_{\mathbb{Z}} \cdot \mathbb{X} \cdot \mathbb{M}_{\mathbb{Z}}\mathbb{Z}\mathbb{M}_{\mathbb{Z}} \cdot \mathbb{X} \cdot \mathbb{M}_{\mathbb{Z}} = -\mathbb{I}\,. \tag{12}$$

The polarization transformation is again proportional to the identity operator, implying a perfect preservation of every input polarization state. In fact, when the effective noise acts along a *known* axis, a complete suppression of decoherence is already obtained by employing only *one* Pauli operator, the one realizing a spin-flip around an axis *orthogonal* to the axis of decoherence.

2.3.2. Pauli-group decoupling for the most general polarization decoherence In the ring-cavity setup, the V and H polarization states are eigenstates of the interaction Hamiltonian of the polarization qubit with its effective environment and are therefore the "pointer states" unaffected by decoherence [30]. In the pointer states basis, decoherence affects only the off-diagonal elements of the polarization density matrix. In the most general case instead, the direction of the pointer state basis in the Bloch–Poincaré sphere is *unknown*. As a consequence in a generic basis, decoherence acts *both* on diagonal and off-diagonal elements of the polarization density matrix. To implement such a generic noise model we have placed in front of each plane mirror a S–B with axis at 45° with respect to the cavity plane. The action of the S–B on the polarization state is described by

$$\mathbb{B}_{\mathbb{X}}(\theta) = \exp(-\mathrm{i}\theta\mathbb{X}/2)\,, \tag{13}$$

where $\mathbb{X} = |H\rangle\langle V| + |V\rangle\langle H|$, and θ is the noise delay-phase. The S-B together with a plane mirror are described by the operator $\mathbb{N}(\omega,\theta)$ like in Eq. (4). The transformation of the polarization state after two round-trips in the presence of the S–Bs is therefore given by:

$$\mathbb{U}_{fe}[\phi(\omega),\theta] = [\mathbb{N}(\omega,\theta)\mathbb{N}(\omega,\theta)] \cdot [\mathbb{N}(\omega,\theta)\mathbb{N}(\omega,\theta)]\,. \tag{14}$$

The free evolution (fe) operator $\mathbb{U}_{fe}[\phi(\omega),\theta]$ can be rewritten as

$$\mathbb{U}_{fe}[\phi(\omega),\theta] = \exp\left[-i\alpha_{fe}(\omega,\theta)\,\vec{s}_{fe}(\omega,\theta)\cdot\vec{\sigma}\right]\,, \tag{15}$$

which describes a rotation in the Bloch–Poincaré sphere of an angle $2\,\alpha_{fe}(\omega,\theta)$ around the direction individuated by $\vec{s}_{fe}(\omega,\theta)$. Therefore by varying θ and the bandwidth of

radiation spectrum, i.e. the distribution of ϕ, one implements the generic polarization decoherence. The rotation angle is given by the implicit expression

$$\sin[\alpha_{fe}(\omega,\theta)/2] = \sin[\phi(\omega)/2]\cos(\theta/2), \tag{16}$$

and

$$\vec{s}_{fe}(\omega,\theta) = \frac{\{\sin\theta[\cos\phi(\omega)-1]\,,\sin\theta\sin\phi(\omega)\,,(1+\cos\theta)\sin\phi(\omega)\}}{2\sin\alpha_{fe}(\omega,\theta)}. \tag{17}$$

Pauli-group decoupling is again realized every two-round trips by adding the BB operations $\mathbb{X}$ (implemented by adding to the noise phase-delay θ of the S–B present in the short arm of the cavity, a further delay of $\lambda/2$) and $\mathbb{Z}$ in the cavity [29, 12]. The overall transformation after the two round-trips for a given frequency component is now given by:

$$\mathbb{U}_{bb}[\phi(\omega),\theta] = [\mathbb{ZN}(\omega,\theta)\mathbb{XN}(\omega,\theta)]\cdot[\mathbb{ZN}(\omega,\theta)\mathbb{XN}(\omega,\theta)]\,, \tag{18}$$

which can be rewritten, as in the free evolution case, as a rotation in the Bloch–Poincaré sphere:

$$\mathbb{U}_{bb}[\phi(\omega),\theta] = \exp[-i\alpha_{bb}(\omega,\theta)\,\vec{s}_{bb}(\omega,\theta)\cdot\vec{\sigma}]\,, \tag{19}$$

with

$$\cos\alpha_{bb}(\omega,\theta) = -(\sin\phi(\omega)\,\sin\theta)/2,$$

and $\vec{s}_{bb}(\omega,\theta)$ defined by the following direction cosines:

$$\begin{aligned}
s_{bb_X}(\omega,\theta) &= [-\sin\phi(\omega)\sin^2(\theta/2)]/[\sin\alpha_{bb}(\omega,\theta)],\\
s_{bb_Y}(\omega,\theta) &= \{1-2\sin^2(\theta/2)\sin^2[\phi(\omega)/2]\}/[\sin\alpha_{bb}(\omega,\theta)],\\
s_{bb_Z}(\omega,\theta) &= \{-\sin\theta\sin^2[\phi(\omega)/2]\}/[\sin\alpha_{bb}(\omega,\theta)].
\end{aligned}$$

The Eq. (19) can be numerically calculated to show that a partial compensation of the general decoherence is obtained through BB control even with this general noise model. This fact has also been experimentally demonstrated [18].

To conclude the section, it is useful to clarify the differences between the two approaches discussed thus far. For that reason, we write once again the two crucial equations Eq. (8) and Eq. (11) which describe the main operator sequences in the two approaches when BB is applied:

$$\text{plane-parallel cavity} \;: \mathbb{M}_{\mathbb{Z}}\mathbb{X}\mathbb{M}_{\mathbb{Z}}^{-1}, \tag{20}$$

$$\text{triangular ring cavity} : \mathbb{Z}\mathbb{M}_{\mathbb{Z}}\mathbb{X}\mathbb{M}_{\mathbb{Z}}. \tag{21}$$

The repetition of both these basic cycles leads to freeze the system dynamics and suppress the detrimental effects of decoherence. In fact, the noise operator is eventually described by an operator proportional to the identity. However the way this is obtained is different in the two approaches.

In the plane-parallel cavity [17], the photon travels *forward* in time on all the odd-numbered trips (i.e. the first, the third, etc.), and retraces its steps *backward* in time on all even-numbered trips. This is evident from the sequence in Eq. (20), where the

noise operator appears once in its direct form and once in its inverse form. Such an approach is then similar to the two-way passive compensation scheme [23], so widely employed in the "plug-and-play" quantum key distribution [3, 31, 32, 33]: it can work only when the communication channel is two-way, i.e. only when the photons carrying the information travel back-and-forth in the channel. Only if this condition is fulfilled the decoherence effects can be suppressed. This is something that must be taken into account for a potential application of the technique.

On the contrary in the triangular ring cavity [18], the noise operator and the rotating elements all appear in their time-forward order. This means that the mirrors of the ring cavity are not effecting a time-reversal of the noise encountered by the light pulse. Hence, there is no need that a photon is reflected back on its path to make this technique work. Such an observation can be useful if BB is going to be applied to one-way communication channels. For instance, the possibility to apply the BB to a single-passage optical fibre is very appealing. In this case, a manufacturing process should be conceived to place the $\mathbb{X}$ and $\mathbb{Z}$ operations equally spaced along the optical fibre in order to implement this kind of BB control.

3. Closed-loop control through active feedback

In this section we describe a closed-loop control conceived to compensate the noise of a communication channel deployed between two users, namely Alice (the transmitter) and Bob (the receiver), who are going to share a piece of information by quantum means. The typical noise considered in this scenario is again the one given in Eq. (3) but without its dependence on the frequency:

$$\mathbb{M}_{\mathbb{Z}} = \exp\left(i\phi\mathbb{Z}\right). \tag{22}$$

The frequency does not play a role in the problem because we consider *monochromatic* polarization qubits only. The condition of a single frequency adopted by the users is quite well accomplished when interferometric filters are inserted in the setup. However, even if the monochromaticity condition is fulfilled, the noise in Eq. (22) can modify the polarization states traveling in the channel, so that receiver's reference system does not coincide with transmitter's anymore. In fact, any state prepared along a direction different from $\mathbb{Z}$ will undergo a rotation around the $\hat{z}$ axis. When this happens, Alice and Bob do not manage to reliably share the desired information anymore.

The kind of noise just described is typical of a Polarization Maintaining (PM) fibre. There, a nonuniform birefringence brings about a preferred direction of propagation, to which are associated the two eigenstates of the operator $\mathbb{Z}$, thus realizing the noise of Eq. (22). Another circumstance where the same kind of noise is encountered is during the phase stabilization of a phase-sensitive interferometer, which is driven away from the zero-noise condition because of the environment's fluctuations in temperature, pressure and other macroscopic quantities. In this case the noise is better known as "phase drift" [21].

Although the frequency-independent noise model of Eq. (22) can appear naive, it applies to a vast number of quantum-based setup [3]. A popular solution for compensating it, is to employ a two-way communication channel which enables a passive compensation scheme in analogy to what already discussed in the previous sections [23, 34]. However this solution cannot work on one-way channels, which are often preferable because of the lower number of channel uses required.

A possible solution working with one-way channels is to transmit a number of reference states specifically conceived to compensate the noise [35]. This requires the interruption of the main communication to allow the transmission of the references. In [36] the reference states are multiplexed, without interruptions, with the signals of the main communication. However, even in this case, there is a waste of resources, committed to the noise compensation issue rather than to the main communication.

In [20] this problem is solved through a real-time monitoring of the Quantum Bit Error Rate (QBER), which is the main figure to be monitored in a typical Quantum Key Distribution (QKD) setup, especially if run with the "BB84" protocol [37]. On the contrary in [21] the same problem is solved via a local monitoring of the *unbalance* in the receiver counts, which is typical of a QKD setup run with the "B92" protocol [38]. However, in both cases, the correction mechanism includes the following crucial elements, depicted schematically in Fig. (2):

- the acquisition of N noisy input, i.e. N states, affected by the channel noise, which is represented by the *misalignment angle* ϕ, which in turn is a function of time;
- the sampling, through the N acquisitions of the previous point, of a quantity $R(\phi)$ ("monitored signal"), which is a function of the time-dependent channel noise ϕ;
- the comparison of $R(\phi)$ with a reference signal $R(0)$, corresponding to the zero-noise setpoint;
- the correction of the detected noise via a local feedback signal. In case of linear feedback, the feedback angle is $\phi_{fb} = A \times [\Delta R(\phi)]$, with $\Delta R(\phi) = [R(0) - R(\phi)]$ and A the gain of the actuator.

The read-and-write procedure just described is performed by Bob in-course-of-action, and can be easily automatized. All the operations can be controlled by a computer which receives the counts from the detectors, estimates the compensation angle for the feedback, and outputs a suitable signal for the actuator.

One crucial question both for the technique described in [20] and the one in [21], is to decide the optimal size of the sample, i.e. of N. This value comes from a tradeoff between a large sample, preferable for increasing the statistics of acquisition, and a small sample, preferable because it minimizes the variation of the noise with the time. The typical situation is depicted in Fig. 3, where a noise increasing linearly with time is considered. Beside the statistical and time-dependent noise there is also an intrinsic background noise that comes from defects in the electronics or from detectors dark counts [36]. If the acquisition time is too large, the noise between two consecutive feedback kicks increases; if too small, the statistical error pertaining to Bob's measurement increases.

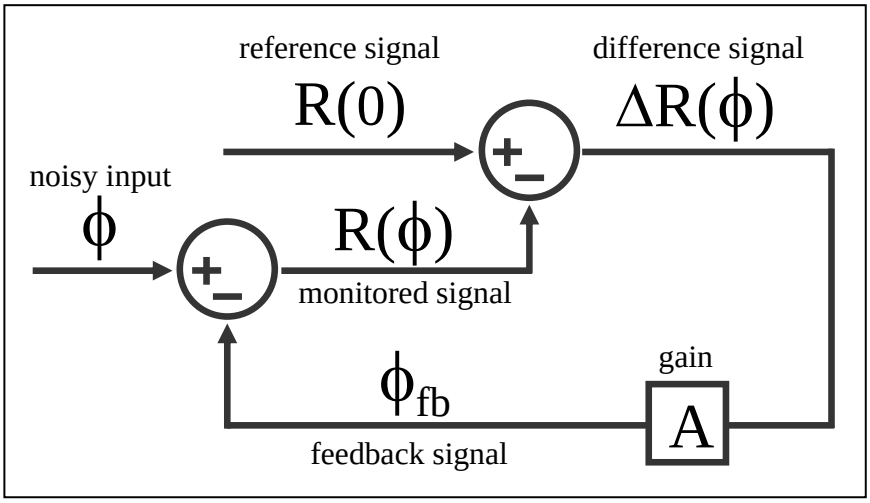

Figure 2. Schematics of the feedback routine.

On the contrary, the noise called "unbiased" in the figure does not play a role in the optimality argument.

The curves of Fig. (3) are drawn based on the typical experimental parameters reported in the literature [35, 36]. They concern the statistical error pertaining to a pure Poisson distribution (curve 'a'), to the distribution of the counts pertaining to Ref. [21] (curve 'b'), and to that pertaining to Ref. [20] (curve 'c'). Hence, the intersections with the misalignment angle $\phi(t)$, linear in time, defines the optimal sampling times in each case.

Let's make explicit the noise dependence on time:

$$\Delta\phi(t) = \phi(t) - \phi(0) = B\Delta t. \tag{23}$$

B is a real constant with the dimensions of the inverse of time and Δt is the amount of time elapsed. On the other side, the non-vacuum states ΔN received in the time unit by Bob are approximately proportional to the transmission rate r of the setup, to its overall transmission coefficient $1-\eta$ and to the average number of photon μ contained in each light pulse:

$$\frac{\Delta N}{\Delta t} = Cr\mu(1-\eta). \tag{24}$$

C is another (positive) constant. Then, if the statistics is not too low, we can approximate the distribution with a Poisson, so that the statistical noise is given by:

$$\frac{\sigma_{\Delta N}}{\Delta N} = \frac{1}{\sqrt{\Delta N}}. \tag{25}$$

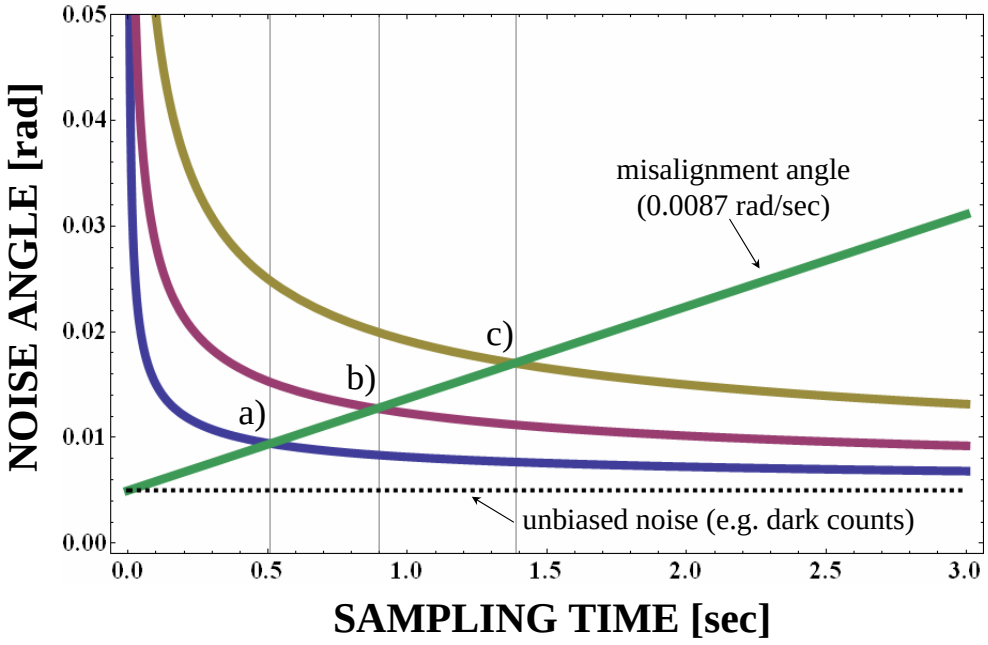

Figure 3. Optimality conditions for the noise in the feedback schemes. a) Case of pure Poisson statistics; b) case of statistics related to the control function of Eq. (35); c) case of statistical noise for a feedback based on the QBER [Eq. (27) and following]. The intersection points are respectively 0.51, 0.90 and 1.39 seconds.

By inserting Eq. (24) into Eq. (25) and equating with Eq. (23) we obtain the optimal sampling time:

$$\Delta t_{opt} = \frac{1}{\sqrt[3]{B^2 C r \mu (1-\eta)}}. \tag{26}$$

By substituting $\frac{\Delta N}{\Delta t} = 10^5$ events/sec and $B = 0.0087$ rad/sec one obtains the value pertaining to the curve 'a' of Fig. (3), i.e. $\Delta t_{opt} = 0.51$ seconds. The other two values are obtained when different monitored functions are taken into account. This is discussed in the next sections.

For our discussion, the monitor function $R(\phi)$ is the main difference between the correction mechanism of Ref. [20] and that of Ref. [21]: the former uses the QBER as a monitor function, while the latter uses the ratio between "inconclusive" and "conclusive" counts, which will be defined later on.

3.1. Closed-loop control with BB84

In Ref. [20] it is shown experimentally the stabilization of a BB84-based QKD session by means of the real-time minimization of the QBER, which results then to be the monitored function:

$$R_{BB84}(\phi) = \text{QBER}. \tag{27}$$

The correction mechanism works at the quantum level and does not require extra resources in addition to those routinely employed for the QKD session.

The BB84 protocols is as follows [37]. Alice prepares at random one of the four quantum states given by $\{|0_x\rangle, |1_x\rangle\}$, eigenstates of $\mathbb{X}$, or $\{|0_y\rangle, |1_y\rangle\}$, eigenstates of $\mathbb{Y}$. The relation between these states is $|0_y\rangle = [(1+\imath)|0_x\rangle + (1-\imath)|1_x\rangle]/2$, $|1_y\rangle = [(1-\imath)|0_x\rangle + (1+\imath)|1_x\rangle]/2$. The users associate the logical bit '0' to the states $|0_x\rangle$ and $|0_y\rangle$, and the logical bit '1' to the states $|1_x\rangle$ and $|1_y\rangle$. Notice that the two sets of states associated to the logical values of the bit are non-orthogonal, i.e. their scalar product is not always zero. This prevents any third party (usually called "Eve"), eavesdropping on the communication channel without authorization, from perfectly distinguishing the two sets of states and so from learning the transmitted bit. This mechanism is at the base of the QKD unconditional security [3]. However, by the same token, the receiver Bob cannot ascertain the bit value as well. To avoid this problem, Bob measures the incoming states along the directions $\mathbb{X}$ or $\mathbb{Y}$, without knowing if the measured state is eigenstate of the former operator or of the latter. Then, after all the qubits have been transmitted by Alice and received by Bob (hence Eve cannot modify them anymore), both Alice and Bob will reveal on public which operators, $\mathbb{X}$ or $\mathbb{Y}$, they have used to prepare the initial qubit (Alice) or to measure the incoming qubit (Bob). This procedure is called "basis revelation". By keeping only those instances in which the bases chosen by the users accidentally coincide (about 50% of the total sample), and discarding all the other instances (remaining 50%), the users are left with only those results which are necessarily correlated, because they descend from the same eigenstate. Hence, the users will take the logical bit associated to the measured eigenstate, either '0' or '1', as a bit of their final key, in principle known to them only (they reveal on public the basis $\mathbb{X}$ or $\mathbb{Y}$, not the value of the measured state).

This procedure works fine in case the communication channel is noiseless. In case of a noisy channel, some errors are present in Bob's outcome. These errors must be corrected to let the users share the same secret key, but they have also a second purpose: the amount of errors found in the communication can be used to put an upper bound to the information stolen by Eve. This upper bound is then used to remove from Eve's hands all the stolen information by means of the Privacy Amplification procedure [39, 40]. Hence, it is very important to quantify the percentage of errors in the sample, i.e. the QBER. The QBER is defined in an operational way as follows:

$$\mathrm{QBER} = \frac{\text{number of errors}}{\text{number of detected events}}, \tag{28}$$

where an error occurs when Alice and Bob, measuring in the same basis, find two different bit values [3]. Notice that Alice and Bob must communicate in order to have an estimate of the QBER, otherwise they cannot know whether they measured in the same basis or not.

It is not difficult to show that the dependence of the QBER from the misalignment angle is the following [35]:

$$\mathrm{QBER}(\phi) = \sin^2(\Delta\phi). \tag{29}$$

At this point we are in the position to note that the use of QBER as a monitored function is not optimal, for several reasons.

First, as already mentioned above, the estimation of the QBER can only be done by Alice and Bob by public discussion, which in turn is realized using the classical authenticated channel, after having completed other operations, like the basis reconciliation for example. While this is not a problem on a dedicated classical channel, it can become critical on a real-world network, where channels are often busy or idle, thus delaying the correction.

Second, in the QBER operative definition, Eq. (28) the numerator is usually much smaller than the denominator. In fact, the QBER must be necessarily lower than 11% to allow unconditional security with BB84 [3], and is usually good to have it around 5%. This means that the sampling ΔN of Eq. (24) is composed by a small percentage of the total counts received by Bob. To be concrete, we can refer to Fig. 3, where we plotted the statistical errors pertaining to an overall rate of $\Delta N = 10^5$ events/sec. To have a QBER around 5%, Bob has to collect samples for an optimal time equal to 1.39 seconds (intersection point of curve 'c'). This corresponds to a total of 1.39×10^5 events, and is the 5% of the total sample, which should then amount to $(1.39 \times 10^5 \times \frac{100}{5})$ i.e. 2.78×10^6 events. This is more than 55 times bigger than the sampling done with the curve 'a' in Fig. (3).

Finally, the statistical error just seen propagates to the estimation of the feedback angle ϕ_{fb}. This is obtained by inverting Eq. (29), after having estimated the QBER Q_{est} from the obtained counts. We then have:

$$\Delta\phi_{fb} = \pm \arcsin \sqrt{Q_{est}}, \tag{30}$$

where the sign of the feedback angle has to be decided by practical random trials. This entails a further factor 2, on the average, for the error descending from it.

By propagating the maximum error we find:

$$d(\Delta\phi_{fb}) = 2 \times \frac{1}{2} \frac{1}{\sqrt{Q_{est}(1 - Q_{est})}}\, dQ_{est} \tag{31}$$

Such an error function is relevant when Q_{est} is small. For instance, the error $d(\Delta\phi_{fb})$ is about 10 times the error dQ_{est} when Q_{est} is about 1%. This is due to the fact that the monitored function, i.e. the QBER, has a nonlinear relation with the feedback angle. In particular, for small values of the QBER, Eq. (29) establishes a quadratic relation with with $\Delta\phi_{fb}$, thus worsening the estimation of the feedback angle.

These inconveniences are avoided when one considers the feedback correction mechanism related to the B92 protocol.

3.2. Closed-loop control with B92

In this section we summarize the correction mechanism introduced in [21] in relation with the B92 protocol. To do so, we introduce the *two* B92 signal states together with the states orthogonal to them:

$$|\varphi_j\rangle = \beta|0_x\rangle + i(-1)^j\alpha|1_x\rangle, \tag{32}$$

$$|\overline{\varphi}_j\rangle = \alpha|0_x\rangle - i(-1)^j\beta|1_x\rangle. \tag{33}$$

In the above equation $|\varphi_j\rangle$ are the signal states and $|\overline{\varphi}_j\rangle$ are the states orthogonal to them, with $j = \{0, 1\}$; $|0_x\rangle$ and $|1_x\rangle$ are the eigenstates of the Pauli operator $\mathbb{X}$; $\beta = \sqrt{1-\alpha^2} = \cos(\theta/2)$ and θ belongs to the open interval $(0, \pi/2)$; i is the imaginary unit. By varying the angle θ the B92 polarization states move in the $\overline{xy}$ plane of the Poincaré sphere.

The B92 protocol works similar to the BB84 protocol described in the previous section. The main difference is that in the B92 only two states, $|\varphi_0\rangle$ and $|\varphi_1\rangle$, directly associated to the bit value '0' or '1', are used for the communication, instead of the four states used in the BB84 protocol. To start the communication, Alice chooses at random the value of the bit j, encodes it in the corresponding state $|\varphi_j\rangle$ and transmits it to Bob. The resulting density matrix ρ prepared by Alice is then:

$$\rho = \frac{1}{2}\left(|\varphi_0\rangle\langle\varphi_0| + |\varphi_1\rangle\langle\varphi_1|\right) = \beta^2|0_x\rangle\langle 0_x| + \alpha^2|1_x\rangle\langle 1_x|, \tag{34}$$

corresponding to a preparation of the state $|\varphi_0\rangle$ in half of the cases and of $|\varphi_1\rangle$ in the other half of the cases. It can be easily verified that the above density matrix is *asymmetric* because it is not proportional to the identity operator in the 2-dimension Hilbert space, $\mathbb{I} = |0_x\rangle\langle 0_x| + |1_x\rangle\langle 1_x|$. This is a consequence of the strict nonorthogonality of the two states of the B92 protocol. To decode the information, Bob measures the incoming states in the basis $\mathbb{B}_k = \{|\varphi_k\rangle, |\overline{\varphi}_k\rangle\}$, $k = \{0, 1\}$. Upon obtaining the state $|\overline{\varphi}_k\rangle$, Bob decodes Alice's bit as $j = k \oplus 1$ (the symbol $\oplus$ means "addition modulo 2") and labels the result as *conclusive*; on the contrary, upon obtaining the state $|\varphi_k\rangle$, Bob is not able to decode Alice's bit deterministically, and simply labels the result as *inconclusive*. This is an example of "negative decoding": the detection of the state $|\overline{\varphi}_0\rangle$, which is orthogonal to the state $|\varphi_0\rangle$, excludes the possibility that Alice prepared $|\varphi_0\rangle$ and compels Bob to acknowledge that Alice must have prepared $|\varphi_1\rangle$. The reasoning is the same if the detected state is $|\overline{\varphi}_1\rangle$. After all the qubits have been sent by Alice and detected by Bob, so Eve cannot alter them anymore, Bob reveals on public which instances resulted in an inconclusive count. The users will then remove all these instances from their string and will be left with only those values which have been deterministically inferred by Bob. This procedure is analogous to the basis revelation in the BB84 protocol. Also for the B92, as for the BB84, it can be defined the QBER of all those events which resulted in a conclusive count. From this parameter, and from the rate of conclusive counts, the unconditional security of the protocol can be assessed [38]. Furthermore, it is possible to use the QBER of the B92 protocol as a control function to drive the feedback correction mechanism, exactly as done with the BB84 protocol. However, we describe in the following a feed-forward correction mechanism which is more efficient than that based on the QBER. It exploits the peculiar asymmetric preparation of the B92 quantum states.

The crucial part of the correction mechanism stems from the observation that when the channel is noiseless, the asymmetric density matrix of Eq. (34) generates different amounts of conclusive and inconclusive counts in each measuring basis of Bob. The expected ratios between the counts in each class can be calculated and is then known to

Bob. When noise acts on the channel, it modifies the statistics of Bob's results so that, by measuring the deviation from the expected quantities, he can quantify the noise and immediately compensate for it.

It should be noted that the density matrix is always diagonal in some basis and cannot correct a noise which is diagonal in the same basis. For example, the density matrix written in Eq. (34) is diagonal in the $\mathbb{X}$ basis, and cannot correct a noise like $\exp(i\alpha\mathbb{X})$. However, Alice can vary the preferred axis of the density matrix after some time, so to cover the whole range of possibilities. This option is left for further analysis in future works.

By fixing $k = 0$ (the choice of the other basis gives analogous results) it is possible to show that the ratio $R(\theta, \phi)$ between inconclusive and conclusive counts in Bob's apparatus is given by [21]:

$$R(\theta, \phi) = \frac{2 + \cos\phi + \cos(2\theta - \phi)}{2 - \cos\phi - \cos(2\theta - \phi)}. \tag{35}$$

$R(\theta, \phi)$ is the control function, or monitored function: it is used to drive the compensation mechanism through an active feedback entirely controlled by Bob without the help of Alice (see Supplementary Material in Ref. [21]).

Contrary to the control function given by the QBER, the curve of $R(\theta, \phi)$ can be very well approximated by its tangent in the zero-noise point, when an optimal angle $\theta_{opt} = \frac{\pi}{3}$ is chosen [21]:

$$R(\frac{\pi}{3}, \phi) = \frac{5}{3} + \frac{8\phi}{3\sqrt{3}} + O(\phi^2). \tag{36}$$

The linear control function of Eq. (36) makes the feedback response very fast, suitable to keep the system aligned in time. Note that such a value of θ is usually considered too big for the B92 protocol. This is true only for the traditional B92 [38] while it results nearly optimal in a new kind of B92 protocol, described in [41].

At this point we can note a few advantages of the present technique.

First, the control is entirely local to Bob, it does not require that the two users communicate at all. This is of practical importance as the classical communications can be quite slow if they do not travel on dedicated channels.

Second, the estimation of the control function is more precise than the one effected through the QBER. This can be seen looking at curve 'b' in Fig. (3) which takes into account the statistical fluctuations of the inconclusive and conclusive counts. When these two quantities are put in ratio to form $R(\theta, \phi)$, the overall statistical noise contains a multiplicative factor $\sqrt{2}$ respect to the curve 'a' in Fig. (3). However, because of the high value of θ, the number of inconclusive and conclusive events are respectively $\frac{5}{8}$ and $\frac{3}{8}$ of the total number of acquired events. So, to have a QBER of about 5%, Bob has to collect samples for an optimal time equal to 0.9 seconds (intersection point 'b' of Fig. (3)) for a total of 0.9×10^5 events. This is the 3/8 of the total sample, which should then amount to $(0.9 \times 10^5 \times \frac{8}{3})$ i.e. 2.4×10^5 events. This is only about 5 times bigger

than the sampling done with the curve 'a' in Fig. (3), and about 10 times smaller than the sampling done with the QBER-based feedback, discussed in the previous section.

Finally, when the feedback angle is calculated by inverting Eq. (36) the error is always less than 10%. This is obtained by evaluating the quality of the approximation with the worst possible angle which allows for a positive gain in the B92, i.e. $\phi_{worst} = 0.2765$ [21]. This means that the statistical error pertaining to the feedback angle ϕ_{fb} is about the same as the control function one. This is in sharp contrast with the QBER-based feedback, where the error related to ϕ_{fb} can be even 10 times bigger than the one pertaining to the control function Q_{est}.

As a final remark, we note that it is possible to choose the control function $R(\theta, \phi)$ in a different way without changing too much the results. For instance, it is often useful to define the control function as the ratio between the conclusive counts in the two different bases of B92 since many experiments are performed with only two detectors arranged in this way. The performances of this new configuration will be analyzed in a future work.

Conclusions

In the present work we have described two different techniques to control the noise of a communication channel affecting the polarization qubit along with the related recent experiments.

The first technique, the open-loop bang-bang control, is entirely passive and allows to correct the polarization decoherence due to the dispersive properties of the medium in which the polarization qubit is propagating. The second technique, the closed-loop feedback control, is active and allows to correct errors due to a misalignment between the distant optical apparatuses of the users.

The two proposed techniques are conceived to correct specifically and separately the two different forms of noise. The open-loop (closed-loop) technique would be ineffective if applied to the noise corrected by the closed-loop (open-loop) technique. In fact, the closed-loop technique cannot increase the purity of a certain state, because it acts only on the final part of the photon's trip, while the polarization decoherence occurs uncontrollably during the photon trip. On the other side, even if the open-loop control created a perfectly noiseless channel, it would not help with the mutual drift brought about by the local environmental conditions of the two distant optical apparatuses. However, the two techniques can be run simultaneously, so to correct both types of noise.

Acknowledgments

We acknowledge fundamental insights brought about by P. Mataloni and G. Vallone. The funding of the EC project FP6-IP-QAP are gratefully acknowledged. M.L. is supported by the 5‰ grant C.F. 81001910439.

References

[1] D. Stucki, N. Walenta, F. Vannel, R. T. Thew, N. Gisin, H. Zbinden, S. Gray, C. R. Towery, and S. Ten, New J. Phys. **11**, 075003 (2009).

[2] R. Ursin, F. Tiefenbacher, T. Schmitt-Manderbach, H. Weier, T. Scheidl, M. Lindenthal, B. Blauensteiner, T. Jennewein, J. Perdigues, P. Trojek, B. Ömer, M. Fürst, M. Meyenburg, J. Rarity, Z. Sodnik, C. Barbieri, H. Weinfurter, and A. Zeilinger, Nat. Phys. **3**, 481 (2007).

[3] N. Gisin, G. Ribordy, W. Tittel, and H. Zbinden, Rev. Mod. Phys. **74**, 145 (2002).

[4] V. Scarani, H. Bechmann-Pasquinucci, N. J. Cerf, M. Dusek, N. Lütkenhaus, and M. Peev, Rev. Mod. Phys. **81**, 1301 (2009).

[5] S. D. Bartlett, T. Rudolph, and R. W. Spekkens, Rev. Mod. Phys. **79**, 555 (2007).

[6] R. Ernst, G. Bodenhausen, and A. Wokaun, *Principles of Nuclear Magnetic Resonance in One and Two Dimensions*, Clarendon Press, Oxford (1987).

[7] G. S. Agarwal, M. O. Scully, and H. Walther, Phys. Rev. Lett. **86**, 4271 (2001).

[8] A. G. Kofman and G. Kurizki, Phys. Rev. Lett. **93**, 130406 (2004).

[9] C. Search and P. R. Berman, Phys. Rev. Lett. **85**, 2272 (2000).

[10] D. Vitali and P. Tombesi, Phys. Rev. A **65**, 012305 (2001).

[11] L.-A. Wu and D. A. Lidar, Physical Review A (Atomic, Molecular, and Optical Physics) **70**, 062310 (pages 8) (2004).

[12] S. Massar and S. Popescu, New Journal of Physics **9**, 158 (2007).

[13] L. Viola, E. M. Fortunato, M. A. Pravia, E. Knill, R. Laflamme, and D. G. Cory, Science **293**, 2059 (2001).

[14] J. J. L. Morton, A. M. Tyryshkin, A. Ardavan, S. C. Benjamin, K. Porfyrakis, S. A. Lyon, and G. A. D. Briggs, Nature Physics **2**, 40 (2006).

[15] E. Fraval, M. J. Sellars, and J. J. Longdell, Physical Review Letters **95**, 030506 (2005).

[16] M. J. Biercuk, H. Uys, A. P. VanDevender, N. Shiga, W. M. Itano, and J. J. Bollinger, Nature **458**, 996 (2009).

[17] A. Berglund, quant-ph/0010001 (2000).

[18] S. Damodarakurup, M. Lucamarini, G. D. Giuseppe, D. Vitali, and P. Tombesi, Phys. Rev. Lett. **103**, 040502 (2009).

[19] D. Vitali, P. Tombesi, and G. J. Milburn, Phys. Rev. Lett. **79**, 2442 (1997).

[20] A. R. Dixon, Z. L. Yuan, J. F. Dynes, A. W. Sharpe, and A. J. Shields, Appl. Phys. Lett. **96**, 161102 (2010).

[21] M. Lucamarini, R. Kumar, G. Di Giuseppe, D. Vitali, P. Tombesi, Phys. Rev. Lett. **105**, 140504 (2010).

[22] M. Lucamarini, G. Di Giuseppe, S. Damodarakurup, D. Vitali, P. Tombesi, arXiv:1101.3739. To appear in Phys. Rev. A (2011).

[23] M. Martinelli, Opt. Commun. **72**, 341 (1989).

[24] R. M. A. Azzam and N. M. Bashara, *Ellipsometry and Polarized Light* (North-Holland, Amsterdam, 1977).

[25] H. Y. Carr and E. M. Purcell, Phys. Rev. **94**, 630 (1954).

[26] L. Viola and S. Lloyd, Physical Review A **58**, 2733 (1998).

[27] L. Viola, S. Lloyd, and E. Knill, Phys. Rev. Lett. **83**, 4888 (1999a).

[28] D. F. V. James, P. G. Kwiat, W. J. Munro, and A. G. White, Phys. Rev. A **64**, 052312 (2001).

[29] L. Viola, E. Knill, and S. Lloyd, Phys. Rev. Lett. **82**, 2417 (1999b).

[30] W. H. Zurek, Rev. Mod. Phys. **75**, 715 (2003).

[31] M. Lucamarini and S. Mancini, Phys. Rev. Lett. **94**, 140501 (2005).

[32] A. Cerè, M. Lucamarini, G. Di Giuseppe, and P. Tombesi, Phys. Rev. Lett. **96**, 200501 (2006).

[33] R. Kumar, M. Lucamarini, G. Di Giuseppe, R. Natali, G. Mancini, and P. Tombesi, Phys. Rev. A **77**, 022304 (2008).

[34] H. Zbinden, J. D. Gautier, N. Gisin, B. Huttner, A. Muller, and W. Tittel, Electron. Lett. **33**, 586

(1997).
[35] V. Makarov, A. Brylevski, and D. R. Hjelme, Appl. Opt. **43**, 4385 (2004).
[36] B. B. Elliott, O. Pikalo, J. Schlafer, and G. Troxel, Proc. SPIE **5105**, 26 (2003).
[37] C. H. Bennett and G. Brassard, Int. Conf. on Comp., Sys. & Sign. Proc., Bagalore, India, 175 – 179 (1984).
[38] C. H. Bennett, Phys. Rev. Lett. 68, 3121 (1992).
[39] C. H. Bennett, G. Brassard, and J. Robert, Siam J. Comput., Soc. Ind. and Appl. Math. **17**, 210 (1988).
[40] C. H. Bennett, G. Brassard, C. Crpeau, and U. M. Maurer, IEEE Trans. Inf. Th. **41**, 1915 (1995).
[41] M. Lucamarini, G. Di Giuseppe, and K. Tamaki, Phys. Rev. A **80**, 032327 (2009).